Separation Science and Technology
Publication details, including instructions for authors and subscription information:
http://www.informaworld.com/smpp/title~content=t713708471

Aggregation in Solvent Extraction Systems Containing a Malonamide, a Dialkylphosphoric Acid and their Mixtures

M. R. Antonio[a]; R. Chiarizia[a]; B. Gannaz[b]; L. Berthon[b]; N. Zorz[b]; C. Hill[b]; G. Cote[c]
[a] Chemistry Division, Argonne National Laboratory, Argonne, Illinois, USA [b] CEA-Valrhô, DEN/VRH/DRCP/SCPS/LCSE, Bagnols-sur-Cèze, France [c] Ecole Nationale Supérieure de Chimie de Paris-ENSCP, Université Pierre et Marie Curie Paris, Paris, France

To cite this Article Antonio, M. R. , Chiarizia, R. , Gannaz, B. , Berthon, L. , Zorz, N. , Hill, C. and Cote, G.(2008) 'Aggregation in Solvent Extraction Systems Containing a Malonamide, a Dialkylphosphoric Acid and their Mixtures', Separation Science and Technology, 43: 9, 2572 — 2605
To link to this Article: DOI: 10.1080/01496390802121537
URL: http://dx.doi.org/10.1080/01496390802121537

Separation Science and Technology, 43: 2572–2605, 2008

ISSN: 0149-6395 print/1520-5754 online
DOI: 10.1080/01496390802121537

Taylor & Francis
Taylor & Francis Group

Aggregation in Solvent Extraction Systems Containing a Malonamide, a Dialkylphosphoric Acid and their Mixtures

M. R. Antonio,[1] R. Chiarizia,[1] B. Gannaz,[2] L. Berthon,[2] N. Zorz,[2] C. Hill,[2] and G. Cote[3]

[1]Chemistry Division, Argonne National Laboratory, Argonne, Illinois, USA
[2]CEA-Valrhô, DEN/VRH/DRCP/SCPS/LCSE, Bagnols-sur-Cèze, France
[3]Ecole Nationale Supérieure de Chimie de Paris-ENSCP, Université Pierre et Marie Curie Paris, Paris, France

Abstract: Aggregation phenomena in *n*-alkane solutions of di-*n*-hexylphosphoric acid (HDHP), *N,N′*-dimethyl-*N,N′*-dioctylhexylethoxymalonamide (DMDOHEMA), and their mixtures, were investigated by electrospray ionization–mass spectrometry (ESI-MS), vapor pressure osmometry (VPO), and small-angle X-ray and neutron scattering (SAXS and SANS). The objective of the study was to probe the formation of mixed HDHP-DMDOHEMA species before and after extraction of trivalent lanthanide and actinide (M^{3+}) nitrates. The most important species formed by HDHP upon metal extraction has the composition $M(DHP)_3(HDHP)_3(H_2O)$. These species exist as spherical aggregates of the reverse micelle type with a polar core diameter of $\sim$7 Å and total diameter of $\sim$11 to $\sim$15 Å. The aggregation of DMDOHEMA is a progressive phenomenon, with an average aggregation number of $\sim$2 in the 0.2 to 0.6 M range and larger aggregates forming at higher concentrations. The metal loaded DMDOHEMA aggregates can be considered as interacting spheres with a polar core diameter

Received 21 October 2007; accepted 12 March 2008.

Address correspondence to R. Chiarizia, Chemistry Divison, Argonne National Laboratory, 9700 South Cass Avenue, Argonne, IL, 60439, USA. E-mail: chiarizia@anl.gov

between ~11 and ~16 Å, depending on composition, a total diameter of up to ~25 Å, and a weight-average aggregation number of ~9. The results obtained in this work provide strong evidence for the formation of mixed aggregates when mixtures of HDHP and DMDOHEMA are used for the extraction of trivalent Ln and An cations. These mixed reverse micelles have a diameter between 19 and 24 Å with a polar core diameter of 10 and to 14 Å. The most recurrent micellar composition is 2 HDHP and either 4 or 5 DMDOHEMA molecules.

Keywords: Am and Eu extraction, aggregation, dialkylphosphoric acids, malonamide, supra-molecular chemistry

INTRODUCTION

In the DIAMEX (Diamide Extraction) – SANEX (Selective Actinide Extraction) solvent extraction process (1), developed by the French Commissariat à l'Energie Atomique (CEA), the separation of the trivalent actinide ions, An(III), from the trivalent lanthanide ions, Ln(III), is accomplished by using a mixture of a diamide and a dialkylphosphoric acid dissolved in an appropriate aliphatic diluent. Under the highly acidic conditions of the aqueous phase, both An(III) and Ln(III) are extracted by the diamide. The separation/recovery of the An(III) is then accomplished in a subsequent step where the An(III) are selectively stripped from the organic phase (2).

The *N,N′*-dimethyl-*N,N′*-dioctylhexylethoxymalonamide (DMDOHEMA, Fig. 1) and the di-*n*-hexylphosphoric acid (HDHP, Fig. 1) are among the possible choices for the extractant mixture for the DIAMEX-SANEX process. The extraction of Ln(III) and Am(III) by the two single extractants and their mixtures in *n*-dodecane under a variety of aqueous and organic phase conditions has recently been investigated (2).

For HDHP, the extraction reaction at tracer concentration level of the metal ions from HNO_3 aqueous solutions can be written as:

$$M^{3+} + 3(\overline{HA})_2 \leftrightarrow \overline{M(A \cdot HA)_3} + 3H^+ \qquad (1)$$

where M^{3+} stands for either Eu^{3+} or Am^{3+}, HA represents HDHP, A is the deprotonated acid, DHP^-, and bars indicate organic phase species (2). In equilibrium 1, HDHP is assumed to be dimeric, consistent with the general behavior of dialkylphosphoric acids in alkane diluents (3,4) and with specific literature information on HDHP (5,6).

For the diamide, also at very low metal concentration, the extraction reaction is:

$$M^{3+} + 3NO_3^- + 2\overline{D} \leftrightarrow \overline{M(NO_3)_3D_2} \qquad (2)$$

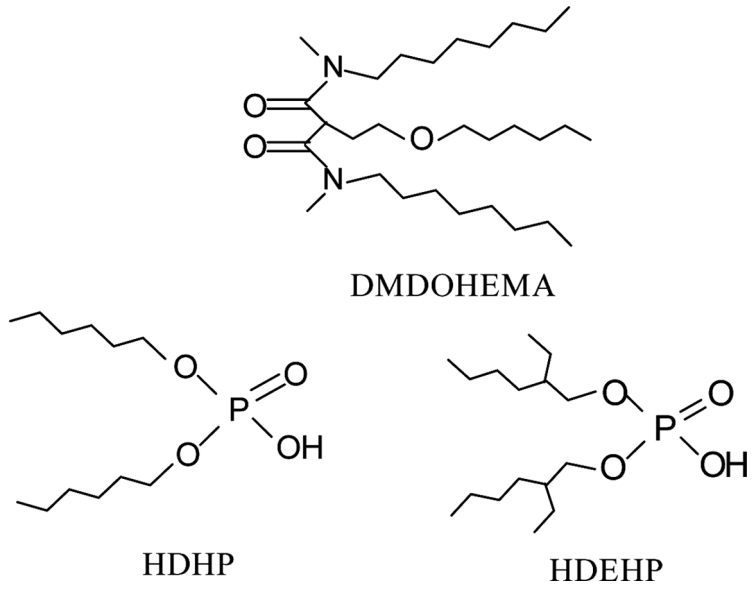

Figure 1. Structures of DMDOHEMA, HDHP and HDEHP.

where D stands for DMDOHEMA (2). The extraction of M^{3+} by DMDOHEMA, however, can be more complex than that shown in equilibrium 2, since nitric acid is coextracted to some extent by the diamide (7), and, at higher metal ion concentrations, higher solvates can be formed (2), e.g., $M(NO_3)_3D_3$. A further complication in the solvent extraction chemistry of diamide reagents in alkane diluents, is the tendency of the extractants to form small aggregates of the reverse micelle type. A three to seven aggregation number for the *N,N′*-dimethyl-*N,N′*-dibutyltetradecylmalonamide (DMDBTDMA) in *n*-dodecane has been reported (8,9,10), depending on the HNO_3 concentration in the aqueous phase.

The extraction of Ln(III) and An(III) by mixtures of the two extractants at constant HDHP concentration in the presence of increasing DMDOHEMA concentrations (2), indicated antagonism in the extraction of Eu^{3+} and synergism in the extraction of Am^{3+}. These data were interpreted as resulting from the formation of mixed HDHP-DMDOHEMA species in the organic phase. The association model that provided results consistent with experiments assumed the formation of a mixed extractant species containing two HDHP and about five DMDOHEMA molecules.

The cation coordination environments in *n*-dodecane solutions containing HDHP, DMDOHEMA or a mixture of the two extractants

loaded with macroamounts of Eu(III) or Am(III), were investigated through extended X-ray absorption fine structure (EXAFS) measurements (11). With HDHP, according to the expectations from equilibrium 1, the cations are coordinated to the six oxygens provided by three monodeprotonated HDHP dimers. With DMDOHEMA, on the other hand, the EXAFS data suggested a metal coordination sphere of eight oxygen atoms, resulting from two bidentate diamide molecules (see equilibrium 2) and a combination of monodentate and bidentate coordination of nitrate ions. Interestingly, the EXAFS data for the organic phase samples containing both extractants, when subjected to principal component analysis, were adequately described as linear combinations of the EXAFS data for the single ligand complexes with HDHP and DMDOHEMA. The data on binary extractant samples, however, could not distinguish between these two possibilities: the two ligands coordinate the cations independently from each other, or, alternatively, they are both involved in the formation of a supramolecular entity in which the cation is bonded to either ligand.

In the present study, we supplemented the molecular level information provided by distribution and EXAFS measurements with further molecular level measurements (electrospray ionization–mass spectrometry, ESI-MS). We also extended our investigation to longer length scales (supramolecular level) through measurements of colligative properties (vapor pressure osmometry, VPO) and small-angle X-ray and neutron scattering (SAXS and SANS). The objective of this work was to investigate the possible formation of mixed HDHP-DMDOHEMA species as suggested by our solvent extraction measurements, to determine the composition of these species and to follow their evolution with changing experimental conditions through independent physico-chemical measurements.

EXPERIMENTAL SECTION

Materials and Procedure

DMDOHEMA, HDHP, di(2-ethylhexyl)phosphoric acid (HDEHP), ^{243}Am, and all other reagents used in this work were the same as described previously (2,11). Equal volumes of the organic phase containing HDHP, HDEHP, DMDOHEMA, or their mixtures in *n*-dodecane were equilibrated in screw-cap tubes at 25°C by vortexing for several minutes, a time sufficient for equilibrium attainment. After centrifugation and phase separation, the organic phases were subjected to the measurements described in this paper. In most cases the conditions were such that practically quantitative extraction of the metal took place. Water

in the organic phases was determined by Karl Fischer titrations using $H_2C_2O_4 \cdot 2H_2O$ as the standard.

ESI-MS Measurements

The investigation of metal-ligand interactions by mass spectrometry (MS) has been very successful since the advent of the electrospray ionization (ESI) technique, which has the ability to preserve and transport metal-ligand complexes from the solution to the gas phase (12–14). An advantage of this technique is its ability to determine the stoichiometry of the complexes in solution and to investigate their stability in the gas phase (15–17). However, despite its advantages, the technique of ESI-MS has been rarely used for solvent extraction studies (18–20).

The mass spectrometry measurements were recorded in the positive ionization mode using a Bruker Esquire-LC quadrupole ion trap equipped with an electrospray interface. The organic phase samples were diluted ten times with ethanol and one thousand times with a water/acetonitrile mixture (50/50) before analysis. A syringe infusion pump (Cole Parmer) delivered the sample at 60 μL/h to the electrospray source. The capillary voltage was set to 4 kV in the positive ionization mode. Nitrogen flowing at 5 L/min was employed as the drying gas, and at 5 psi as the nebulizing gas. The source temperature was set to 250°C. The sample cone voltage was optimized at 30 V. Spectra were acquired over an m/z (mass to charge ratio) range of 45–2200. The energy resolved mass spectrometry experiments were performed by varying the cone voltage (skimmer 1) between 20 to 100 V, with the skimmer 2 voltage kept constant at 10 V.

VPO Measurements

Vapor pressure, a colligative property, is directly related to the number of particles in solution. Therefore, vapor pressure measurements are often used to investigate aggregation phenomena. The VPO measurements on solutions of the extractants were performed using a Knauer K-7000 vapor pressure osmometer as described previously (9). The measurements were performed at various temperatures depending on the diluent used (60, 40, and 24°C for *n*-dodecane, *n*-heptane and *n*-pentane, respectively). 1-Bromotetradecane or tri-*n*-octylamine was used as monomeric reference materials. The aggregation equilibria established in solution were identified by writing the number-average aggregation number, n_{av}, as:

$$n_{av} = \frac{C_{tot}}{S} = \frac{C_{tot}}{\Delta V / K_r} \tag{3}$$

where C_{tot} is the analytical concentration of the extractant, S is the sum of the concentrations of each species present in the system, ΔV (in mV) is the osmometer instrumental reading, and K_r is the calibration constant obtained from the measurements with the monomeric standard. C_{tot} and S were expressed through the following mass balance equations and aggregation equilibrium constants (β_n):

$$C_{tot} = a + n \sum \beta_n a^n \quad (4)$$

$$S = a + \sum \beta_n a^n \quad (5)$$

where "a" represents the monomer concentration. The calculation of n_{av} and corrections from non-ideal behavior of the solutes were performed following published procedures (9,21,22).

SAXS and SANS Measurements

X-ray and neutron scattering measurements are ideally suited for the investigation of the morphology (shape and size) of particles of the reverse micelle type, i.e., particles that have a polar core where polar, inorganic solutes are confined, and a hydrophobic shell, where the lipophilic alkyl chains of the extractant(s) are located. The SAXS measurements highlight the polar core of the particles, characterized by a different electron density than the bulk solution. In contrast, SANS measurements for samples prepared in a deuterated diluent highlight the whole particle by taking advantage of the different nuclear properties of the D atoms in the diluent and the H atoms in the hydrophobic shell. The combined information from both techniques, therefore, should provide a complete picture of the particle morphology.

Data Collection

SAXS data were collected at beam lines 12-BM-B (23) and 12-ID-C (24) of the Advanced Photon Source at Argonne National Laboratory with an incident photon energy of 18.0 keV, which was chosen to provide good transmittance through the cells and, at the same time, to be just high above the L-edge energies of Ce, Nd, and Eu, and below the Am L_3-edge energy. Solutions without Am were contained in thin-layer (1.7 mm path length), small volume (*ca.* 20 μL), parallel-plate cells fabricated of PCTFE with optically transparent PCTFE film windows of 0.010" thickness (Boyd Technologies, Inc.). The Am solutions were contained in larger PCTFE cells (6 mm path length and 1 mL capacity) of parallel-plate

design with optically transparent PCTFE film (0.010") windows (Boyd Technologies, Inc.). Because both HDHP and DMDOHEMA alone and in combination effectively wet and, over the course of several weeks time, penetrate PCTFE, all cells containing Am solutions were encapsulated in heat-sealable bags. The 2-D scattering profiles were recorded with a MAR-CCD-165 detector (on 12-BM-B) and a 9-segment CCD Gold detector (on 12-ID-C) (24). The sample-to-detector distances were adjusted to provide a detecting range for momentum transfer of $0.02 < Q \leq 1\,\text{Å}^{-1}$, where Q, the momentum transfer, was calibrated using a silver behenate standard. After correction for spatial distortion and detector sensitivity, the 2-D scattering images were azimuthally averaged to produce plots of scattered intensity, I(Q) (cm^{-1}) vs. Q, where $Q = (4\pi/\lambda)\ \sin(\theta)$ ($Å^{-1}$), in which θ is half the scattering angle and λ is the X-ray wavelength, following standard procedures (25,26). The background response was removed in identical fashion, involving the subtraction of the empty cell scattering and the scattering arising from the diluent, i.e., (dodecane – empty cell) × (solvent volume fraction). The sample identifications and compositions are provided in Table 1.

The SANS measurements were performed at the time-of-flight small-angle neutron diffractometer (SAND) at the Intense Pulsed Neutron Source of Argonne National Laboratory (27). The samples were measured in standard Suprasil cells with a pathlength of 2 mm, a sample volume of 0.8 mL, and data collection time of four hours. For each sample, the data were collected as scattered intensity, I(Q) (cm^{-1}) vs momentum transfer, $Q = (4\pi/\lambda)\ \sin(\theta)$ ($Å^{-1}$), where λ, in this case, is the wavelength of the probing neutrons. The samples for SANS measurements were prepared by using deuterated *n*-dodecane as the diluent. Deuterated HDHP was used for selected samples. The absolute intensity of the scattering data was obtained using as secondary standards polymer and porous silica samples with known cross sections, following the procedure reported previously (28). The composition of the samples is shown in Table 2.

Data Interpretation

For the interpretation of the small-angle X-ray or neutron scattering results, the following equation describing scattering by a monodisperse system of particles was used:

$$I(Q) = N_p\, V_p^2\, (\rho_p - \rho_s)^2\, P(Q)\, S(Q) + I_{inc} \qquad (6)$$

where I(Q) is the intensity of the X-ray or neutrons scattered by the solute particles (obtained from the experimental intensities by subtracting the

Table 1. Composition of samples for SAXS measurements and results from data fit using a polydisperse interacting sphere model. Diluent: *n*-dodecane. T = 24 ± 1°C.

Sample #	[HDHP] M	[DMDO-HEMA] M	[HNO_3] M	[H_2O] M	Cation	[M^{3+}] M	d_p[a] Å	Polydis-persity Å
1	0.3	0	0.020	0.057	/	0	7.4	0.1
2	0.3	0	0	0.074	/	0	7.5	0.2
3	0.3	0	0	0.064	Am	0.01	5.8	0.5
4	0.3	0	0	0.064	Eu	0.01	6.1	0.2
5	0.3	0	0	0.064	Eu	0.05	8.3	0.2
6	0	0.7	0.44	0.52	/	0	14.2	3.1
7	0	0.7	0	0.36	/	0	10.8	0.9
8	0	0.7	0	0.40	Eu	0.005	12.2	1.3
9	0	0.7	0.46	0.57	Nd	0.01	11.8	2.7
10	0	0.7	0.46	0.60	Am	0.01	11.3	2.0
11	0.3	0.7	0	0.52	/	0	11.1	3.1
12	0.3	0.7	0.20	0.67	/	0	12.6	3.5
13	0.3	0.7	0.47	0.88	/	0	13.7	4.3
14	0.05	0.7	0	0.27	/	0	10.5	0.3
15	0.3	0.05	0.052	0.12	/	0	9.0	0.3
16	0.3	0.7	0	0.33	Nd	0.01	10.6	1.6
17	0.3	0.7	0	0.37	Nd	0.05	10.0	2.9
18	0.3	0.7	0	0.29	Nd	0.1	10.1	2.9
19	0.3	0.7	0.60	0.81	Nd	0.01	14.1	4.0
20	0.3	0.7	0	0.35	Am	0.01	10.1	0.3
21	0.3	0.7	0.20	0.60	Am	0.01	13.0	2.6
22	0.3	0.7	0.47	0.81	Am	0.01	13.9	3.2
23	0.3	0.7	0	0.46	Ce	0.009	10.8	2.9
24	0.3	0.7	0.47	0.81	Eu	0.009	13.3	3.9

[a]polar core diameter; uncertainty: ± 10%

Table 2. Composition of samples for SANS measurements and results from data fit using Baxter model. Diluent: *n*-dodecane. $T = 24 \pm 1\,^{\circ}C$.

Sample #	[HDHP] M*D-HDHP	[DMDO-HEMA] M	$[HNO_3]$ M	[H_2O] M *D_2O	Cation	$[M^{3+}]$ M	d_{hs}[a] Å	d_p[b] Å	$n_{w,av}$[c] HDHP	$n_{w,av}$[c] DMDO-HEMA	U(r)[d] k_BT
1	0.3	0	0	0.074	/	0	11.4	5.6	1.7	/	-2.4
2	0.3	0	0	0.064	Nd	0.025	15.1	6.8	4.0	/	-2.6
3	0	0.7	0.44	0.52	/	0	27.2	17.8	/	12	-2.6
4	0	0.7	0.46	0.57	Nd	0.01	25.1	16.5	/	8.8	-2.4
5	0.3	0.7	0	0.29	Nd	0.1	20.6	12.3	1.8	4.2	-2.4
6	0.3	0.7	0.2	0.54	Nd	0.1	23.9	14.9	2.7	6.4	-2.8
7	0.3	0.7	0	0.33	Nd	0.01	19.4	11.5	1.5	3.6	-2.3
8	0.3	0.7	0	0.36	Nd	0.025	20.5	12.2	1.8	4.2	-2.8
9	0.3	0.7	0	0.37	Nd	0.05	20.8	12.4	1.9	4.4	-3.1
10	*0.3	0.7	0	0.29	Nd	0.1	21.4	12.9	/	5.9	-2.9
11	*0.3	0.7	0	*0.29	Nd	0.1	23.7	14.3	/	8.1	-2.1
12	0.3	0.05	0	0.068	Nd	0.05	14.0	7.1	2.4	0.40	-2.0
13	0.3	0.3	0	0.13	Nd	0.05	16.7	9.5	1.8	1.8	-1.9
14	0.1	0.7	0	0.27	Nd	0.05	18.1	11.1	0.47	3.3	-1.9
15	0.3	0.7	0	0.46	Ce	0.01	20.6	12.3	1.8	4.2	-3.0
16	0.3	0.7	0	0.36	Nd	0.1	21.6	12.9	2.1	4.9	-2.6

[a]hard sphere diameter; uncertainty $\pm$ 5%
[b]polar core diameter; uncertainty $\pm$ 10%
[c]weight-average aggregation number; uncertainty $\pm$ 10%
[d]energy of attraction between particles; uncertainty $\pm$ 10%.

intensities measured for the diluent alone), N_p is the number of scattering units per unit volume, V_p is the particle volume, $(\rho_p\text{-}\rho_s)^2$ is the contrast factor (determined by the difference in electron density or the scattering length density of particles and solvent for SAXS and SANS data, respectively), P(Q) is the single particle form factor, which describes the angular scattering distribution as a function of particle size and shape, S(Q) is the structure factor, which accounts for interactions between the scattering particles, and I_{inc} is the scattering background (29).

The background-subtracted I(Q) vs. Q SAXS data were fit using various models, including ellipsoid, cylinder, and sphere models with Igor Pro 5.01 (Wavemetrics, Inc.) and IPNS SAS macros. The best fits were obtained by using a polydisperse interacting sphere model, which assumes a spherical shape for the particles, with an adjustable diameter of the polar core, d_p, and polydispersity, listed in Table 1. The polydispersity values are relatively small, with an average of $\pm 15\%$ over all the samples investigated.

For the interpretation of the SANS data, the particles were assumed to be spherical and the evaluation of the extent of interaction between particles was performed using the Baxter model for hard spheres with surface adhesion, following the procedure described previously (30,31). According to this model, an approximate value of the potential energy of attraction (negative) between two hard spheres, U(r), expressed in k_BT units, is given by the following equation:

$$U(r) = \lim_{\delta \to d_{hs}} \ln\left[12\tau\left(\frac{\delta \quad d_{hs}}{d_{hs}}\right)\right] \tag{7}$$

where d_{hs} is the diameter of the hard spheres and $(\delta\text{-}d_{hs})$ represents the width of a narrow square attractive well. The parameter τ in eq. 7 is the reciprocal of the "stickiness parameter," τ^{-1}, and its value increases directly with the strength of the attraction between particles. The Baxter model provides analytical expressions for the structure factor, S(Q), in eq. 6 (30). The fit of each set of experimental data to eq. 6 according to the Baxter model was done by using d_{hs}, τ and I_{inc} as fitting parameters. For simplicity, based on the results from the SAXS measurements, the particles were assumed to be monodisperse spheres, which greatly simplifies the fitting procedure. It is likely, however, that a similar average level of polydispersity ($\pm 15\%$) also exists for the SANS samples. The interparticle attraction potential energy, U(r), was calculated using eq. 7 with an extremely narrow attractive well, i.e., with a width equal to 10% of the particle diameter ($(\delta\text{–}d_{hs})/d_{hs} = 0.1$). The main results from the fits of the SANS data are shown in Table 2.

RESULTS AND DISCUSSION

HDHP

ESI-MS

The extraction of europium and neodymium was studied using two dialkylphosphoric acids: di(2-ethylhexyl)phosphoric (HDEHP, Fig. 1) and di-*n*-hexylphosphoric acid (HDHP). A complete discussion of the organic phase species, based on a combination of mass spectrometry data, molecular dynamic simulations and quantum chemistry calculations, has been reported elsewhere (20).

From the ESI-MS data, three species have been identified for both extractants, i.e., $[LnA_2(HA)_2]^+$, $[LnA_2(HA)_3]^+$ and $[LnA_2(HA)_4]^+$ (where HA and A represent the undissociated dialkylphosphoric acid and its anion, respectively), with $[LnA_2(HA)_2]^+$ being the most stable species in the gas phase. The solution behavior of the two dialkylphosphoric acids is similar, as they both form the neutral $LnA_3(HA)_3$ complex. During the ionization process and the transfer into the gas phase, this neutral species is transformed into $[LnA_2(HA)_4]^+$ by the addition of a proton to form a positive ion. The fragmentation of this ion shows

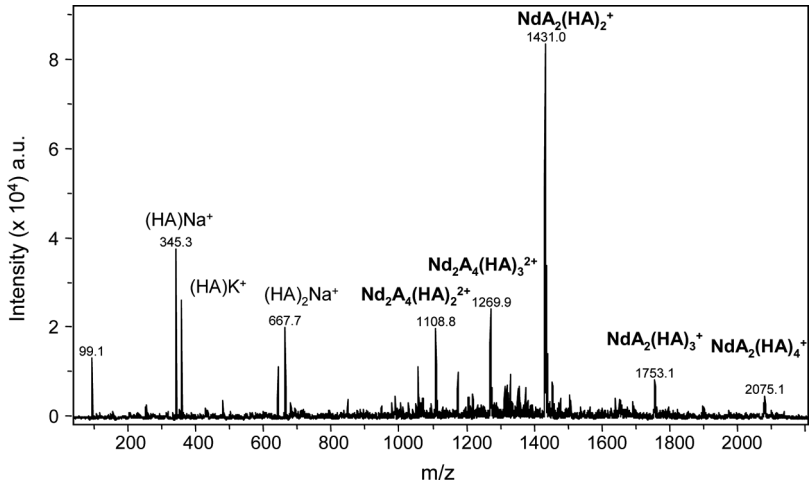

Figure 2. Positive ESI mass spectrum for 0.1 M HDEHP in *n*-dodecane after equilibration with 1 M $Nd(NO_3)_3$ in 0.1 M HNO_3. AH represents HDEHP. The peak at $m/z = 99.1$ is assigned to protonated H_3PO_4 arising from fragmentation of HDEHP during the ionization process; the peaks at $m/z = 345.3$; 361.3; 645.6; 667.7 are assigned to $[(HA)Na]^+$, $[(HA)K]^+$, $[(HA)_2H]^+$, and $[(HA)_2Na]^+$, respectively.

that two ligands are less strongly bonded to the metal and the more stable species in the gas phase is $[LnA_2(HA)_2]^+$.

To supplement this study, an experiment was performed in which a 0.1 M HDEHP solution in *n*-dodecane was equilibrated with a 0.1 M HNO_3 aqueous solution containing a large excess of $Nd(NO_3)_3$ in order to achieve organic phase saturation. The ESI-MS results in Fig. 2 show that the most abundant species in the gas phase was the $[NdA_2(HA)_2]^+$ ion. However, the presence of $[NdA_2(HA)_3]^+$ and $[NdA_2(HA)_4]^+$ with a lower intensity, and of dinuclear species such as $[Nd_2A_4(HA)_x]^{2+}$ with $x = 2$ or 3 was also observed. The formation of dimeric species in the extraction of Nd(III) by HDEHP at high loading of the organic phase was reported earlier (32).

VPO

The VPO measurements were made on up to 0.6 M HDHP solutions in *n*-pentane at 24°C. Before the measurements, the organic solutions were first equilibrated with water, or 0.1 M HNO_3, in the absence and in the presence of increasing $Ce(NO_3)_3$ concentrations (in the 0.01 to 0.1 M range). The results obtained after equilibration with water were interpreted with an aggregation model involving formation of dimers, trimers and tetramers, with the dimer being the most important species, followed by the tetramer at the highest HDHP concentrations ($\beta_2 = 1.6 \cdot 10^2$, $\beta_3 = 1.6 \cdot 10^2$, $\beta_4 = 1.0 \cdot 10^5$). The presence of HNO_3 in the aqueous phase caused a modest increase of the number-average aggregation number, n_{av}.

The VPO data obtained after extraction of macroconcentrations of Ce^{3+} showed a pronounced increase of the extractant average aggregation number, n_{av}, with an increase of the concentration of extracted metal. At all extractant concentrations, a limiting value of $n_{av} = 6$ was reached when the $[HDHP]/[Ce]_{org}$ ratio approached six. Under these conditions, water analysis in the organic phase revealed that the concentration of water was close to that of the metal. These results led to the conclusion that the $Ce(DHP)_3(HDHP)_3(H_2O)$ species predominates at high loading of the organic phase, although smaller aggregates exist in solution ($n_{av} < 6$) when the extractant is in large excess over the extracted metal.

SAXS

0.3 M HDHP in *n*-dodecane was equilibrated with 0.1 or 3 M HNO_3, or loaded with Am^{3+} or Eu^{3+} from 0.1 M HNO_3. The SAXS data for these organic phases were best fit using a polydisperse interacting sphere

model. In all cases the diameter of the polar core, d_p, of the spheres (to be regarded as reverse micelles) was ~ 7 Å, with only small changes with the concentration of solutes in the organic phase (see Table 1, samples 1 through 5). The polar core of the micelles is thought to contain the polar solutes, such as water, nitric acid, metal nitrate, and the $O_3P(O)(OH)$ group of the extractant. Fig. 3a shows the data and the fit for the Am containing sample 3 in Table 1.

SANS

SANS measurements were made for 0.3 M HDHP solutions in deuterated *n*-dodecane after equilibration with 0.1 M HNO_3 in the absence and in the presence of Nd^{3+} (see samples 1 and 2 in Table 2). The data, interpreted using the Baxter model, showed that the HDHP aggregates have a weight-average aggregation number, $n_{w,av}$, of ~ 2 in the absence of metal, and of ~ 4, after Nd extraction. Metal extraction brings about a significant increase of the particle diameter (d_{hs} from ~ 11 to ~ 15 Å). However, d_p, the diameter of the polar core, remains between 6 and 7 Å, in agreement with the results from the SAXS measurements.

Fig. 3b shows the data and the Baxter model fit for sample 2. It is interesting to observe that the energy of attraction between particles, U(r), reached a value as high as $-2.6\,k_BT$, which is close to the value generally observed when the critical point of organic phase splitting (third phase formation) is approached (8,9,31,33–36). The proximity of sample 2 to the phase splitting condition is probably the reason why the SANS data in Fig, 3B exhibit an increase in intensity for very low Q values (< 0.01 Å^{-1}).

DMDOHEMA

ESI-MS

The ESI-MS data for a 0.65 M DMDOHEMA solution in *n*-dodecane, after equilibration with an aqueous solution containing 0.1 M $Nd(NO_3)_3$, 1 M HNO_3 and 2 M $LiNO_3$ exhibited peaks corresponding to several Nd-diamide species, with 2 to 7 diamide molecules for each metal center (Fig. 4a, where D stands for DMDOHEMA).

To gain information about the stability of theses species, energy resolved mass spectrometry experiments with cone voltage variation were performed. The results showed that the most abundant and stable species is $[NdD_4]^{3+}$. Indeed, the intensity of ions such as $[NdD_x]^{3+}$ with $x \geq 5$ strongly decreases with an increase of the cone voltage (Fig. 4b). These

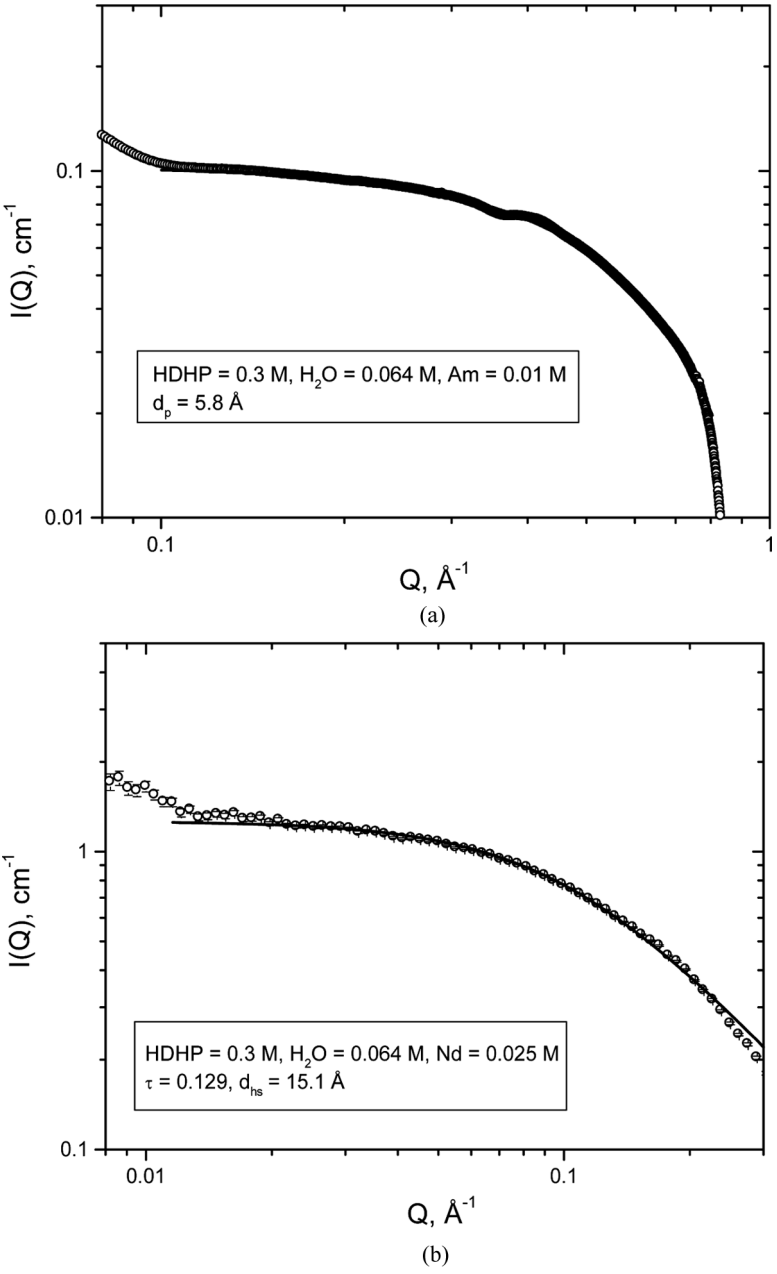

Figure 3. A. SAXS data and interacting spheres fit for Am^{3+}-HDHP in *n*-dodecane (sample 3 in Table 1). B. SANS data and Baxter model fit for HDHP sample 2 in Table 2 (diluent: deuterated *n*-dodecane).

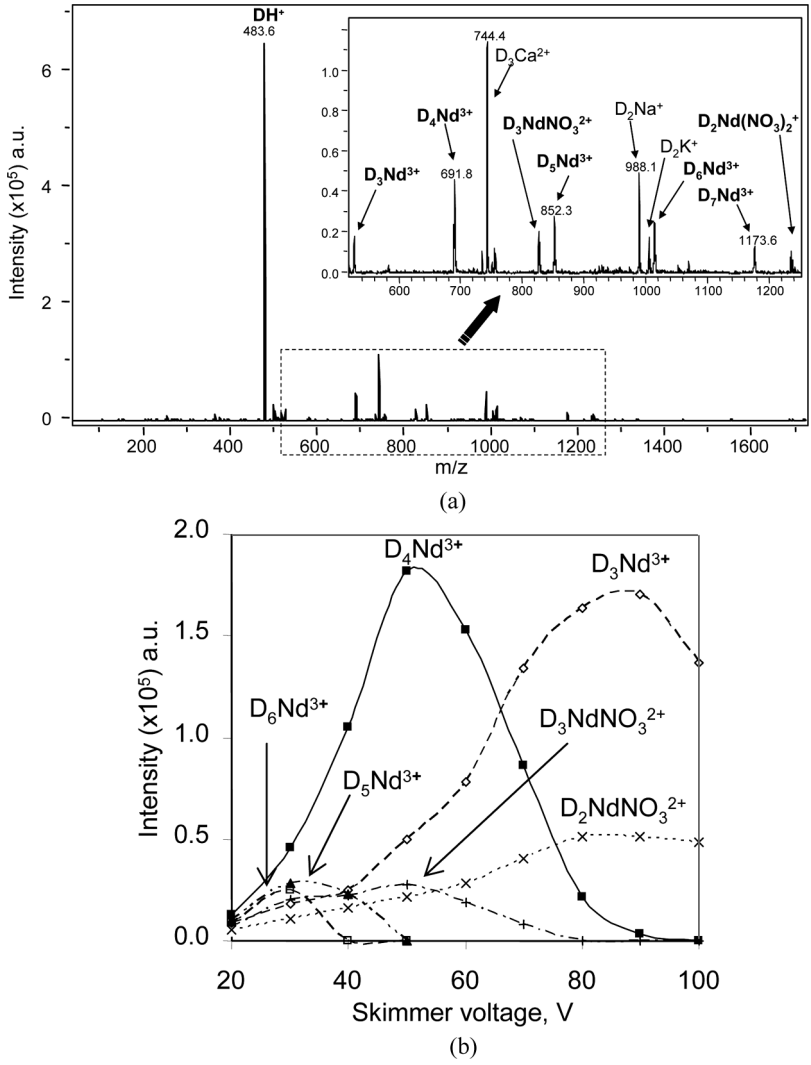

Figure 4. A. Positive ESI mass spectrum for 0.65 M DMDOHEMA in *n*-dodecane after equilibration with 0.1 M $Nd(NO_3)_3$ in 1 M HNO_3 + 2 M $LiNO_3$. D stands for DMDOHEMA. B. Intensity of Nd-diamide ions as a function of cone voltage for 0.65 M DMDOHEMA in *n*-dodecane after equilibration with 0.1 M $Nd(NO_3)_3$ in 1 M HNO_3 + 2 M $LiNO_3$. D stands for DMDOHEMA.

species are not very stable and are probably formed during the ionization process. The intensity for the $[NdD_4]^{3+}$ species is maximum at a skimmer voltage of 50 V. Further increase of the cone voltage leads to its fragmentation by loss of a malonamide molecule and formation of $[NdD_3]^{3+}$.

From theses results it appears that the neutral complexes formed in the organic phase are of the $Nd(NO_3)_3D_x$ type with $2 \leq x \leq 4$, the most abundant being the $Nd(NO_3)_3D_4$ species. During the ionization process and transfer into the gas phase, these species are changed into $[Nd(NO_3)_2D_x]^+$, $[Nd(NO_3)D_x]^{2+}$, and $[NdD_x]^{3+}$.

VPO

VPO measurements made on DMDOHEMA solutions in *n*-dodecane at 60°C, *n*-heptane at 40°C, and *n*-pentane at 24°C consistently indicated that the diamide is monomeric up to $\sim$0.2 M, exhibits an average aggregation number of $\sim$2 in the 0.2 to 0.6 M range, and forms aggregates with a n_{av} value of $\sim$4 at higher concentrations. In all cases, solute aggregation proceeds stepwise, thus making it difficult to assume for this system the existence of a critical micelle concentration, cmc. Water analyses and VPO measurements on the DMDOHEMA-pentane system at 24°C after equilibration with water showed that the water concentration in the organic phase increased steeply after the onset of aggregation. This suggests that water is mainly extracted by the aggregates, and likely reports into the polar core of reverse micelles.

Upon extraction of either HNO_3 or $Ce(NO_3)_3$ by DMDOHEMA in *n*-pentane, a strong increase of n_{av} was observed. This is shown in Fig. 5 where the n_{av} values are reported as a function of the diamide concentration after equilibration with 3 M HNO_3 (panel A), and after extraction of progressively increasing amounts of $Ce(NO_3)_3$ from 3 M HNO_3 (panel B). The data in Fig. 5a clearly show that nitric acid has a much stronger effect than water on the aggregation of DMDOHEMA. At the same time, water analyses indicated that the extraction of HNO_3 is accompanied by a significant increase of water extraction into the organic phase. This result is probably due to the swelling of the polar core of DMDOHEMA reverse micelles following nitric acid extraction. The data in Fig. 5b indicate a further increase of the diamide aggregation number (up to $n_{av} > 6$) when macroconcentrations of metal nitrates are extracted (the highest organic phase Ce concentration in Fig. 5b was 0.066 M).

SAXS

0.7 M DMDOHEMA in *n*-dodecane was equilibrated with aqueous phases containing 3 M HNO_3 (or 3 M $LiNO_3$) in the absence and in the presence of macroconcentrations of europium, neodymium or americium nitrates (samples 6 through 10 in Table 1). The SAXS data were interpreted using the same model of polydisperse interacting spheres

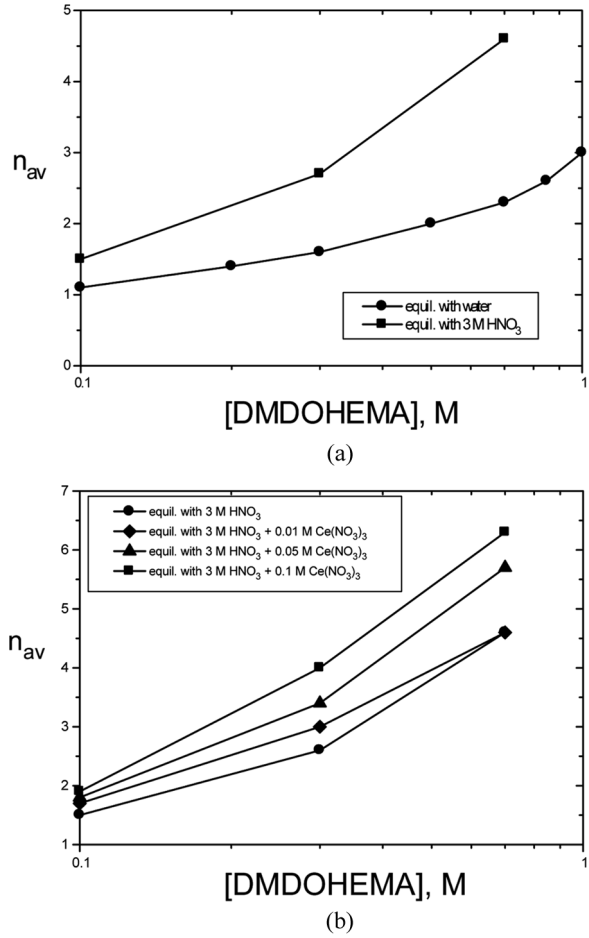

Figure 5. A. Number-average aggregation number, n_{av}, for DMDOHEMA in *n*-pentane after equilibration with water or 3 M HNO_3 at 24°C. B. n_{av} for DMDOHEMA in *n*-pentane after equilibration with 3 M $HNO_3 + 0$, 0.01, 0.05 or 0.1 M $Ce(NO_3)_3$ at 24°C.

as for the HDHP samples. Fig. 6a shows the data and the fits for samples 7 and 8.

The diameter of the polar core of the aggregates, containing water, nitric acid, metal nitrate, and the polar portion of the extractant molecules, is $\sim$14 Å when the diamide is equilibrated with 3 M HNO_3 in the aqueous phase (sample 6), but decreases to $\sim$11 Å when HNO_3 is replaced by $LiNO_3$ (no HNO_3 in the organic phase, sample 7). Extraction

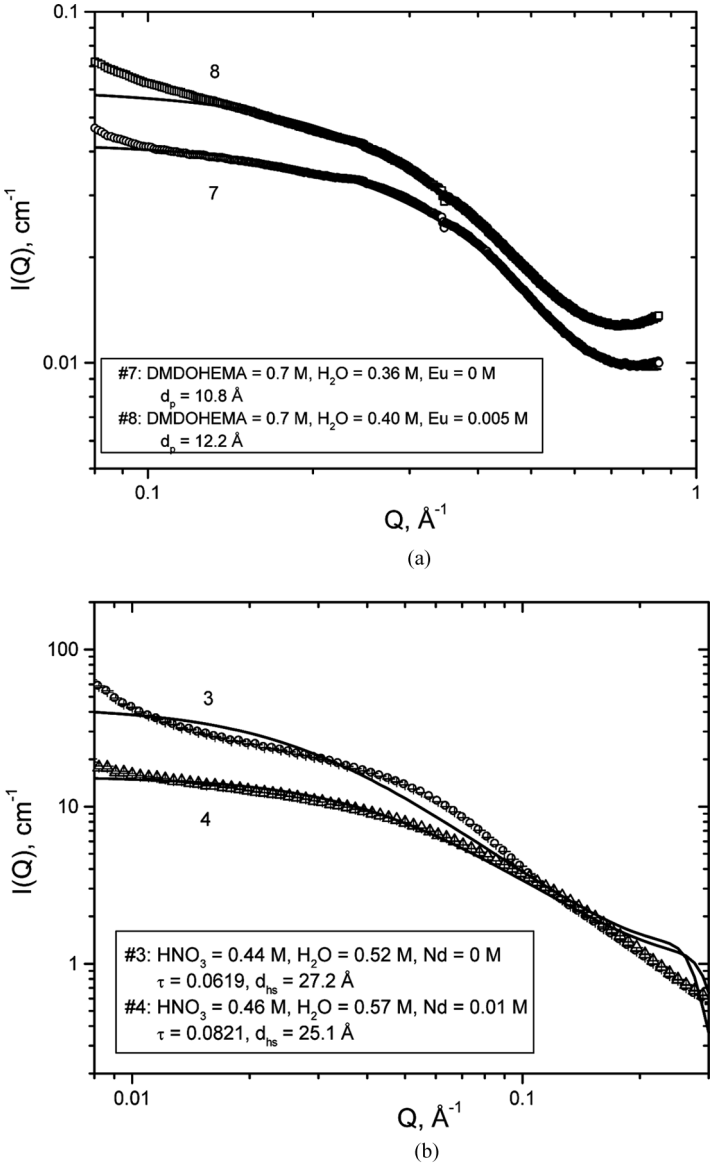

Figure 6. A. SAXS data and interacting spheres fit for 0.7 M DMDOHEMA in *n*-dodecane after equilibration with 3 M $LiNO_3$ with or without $Eu(NO_3)_3$ (samples 7 and 8 in Table 1). B. SANS data and Baxter model fit for 0.7 M DMDOHEMA in deuterated *n*-dodecane after equilibration with 3 M HNO_3 with or without $Nd(NO_3)_3$ (samples 3 and 4 in Table 2).

of metal nitrates from 3 M HNO_3 is accompanied by a contraction of the polar core ($d_p = 11$ to 12 Å, samples 9 and 10), whereas metal extraction from 3 M $LiNO_3$ is followed by modest polar core swelling ($d_p = \sim 12$ Å, sample 8 and Fig. 6a).

SANS

SANS measurements were made for 0.7 M DMDOHEMA solutions in *n*-dodecane (deuterated) after equilibration with 3 M HNO_3 in the absence and in the presence of $Nd(NO_3)_3$ (samples 3 and 4 in Table 2). Fig. 6b shows the data and the Baxter model fit for these samples. The fit for sample 3 is poorer than that for sample 4. The SANS data for both samples share common features, i.e., oscillations at high Q and increased intensities at very low Q values. The high Q oscillations are due to the spherical form factor (37) (P(Q) in eq. 6) used for the Baxter model calculations. For simplicity, the calculations were performed for a single particle size. Introduction of particle polydispersity would eliminate the oscillations. As previously mentioned for the HDHP data, the increased intensity at low Q values is caused, at least in part, by the presence in solution of microscopic heterogeneities which in turn are due to the proximity of the extraction system to the critical condition for phase splitting.

The SANS data, interpreted according to the Baxter model, indicate that the reverse micelles formed by DMDOHEMA after extraction of water and HNO_3 are relatively large, with a hard sphere diameter of ~ 26 Å, a polar core diameter of ~ 17 Å (which compares with ~ 14 Å from SAXS data), and a weight-average aggregation number of 12. Note that the discrepancy between the d_p values from SAXS and SANS data largely disappears when the polydispersity in the SAXS results is taken into consideration. The SANS data obtained after extraction of $Nd(NO_3)_3$ from 3 M HNO_3 confirm the results from the SAXS measurements: metal extraction is accompanied by a decrease in overall size, polar core diameter and aggregation number of the micelles.

HDHP-DMDOHEMA Mixtures

ESI-MS

For the ESI-MS measurements, two dialkylphosphoric acids, HDHP or HDEHP, were used in mixtures with DMDOHEMA. Solutions containing 0.3 M HDHP or HDEHP and 0.65 M DMDOHEMA in *n*-dodecane were used to extract Nd^{3+} from two different aqueous solutions: 0.1 M $Nd(NO_3)_3 + 0.1$ M HNO_3, or 0.1 M $Nd(NO_3)_3 + 1$ M

$HNO_3 + 2\,M\ NaNO_3$. Organic phase samples for the ESI-MS tests were prepared in the same way as for the single extractant systems. For the HDHP-DMDOHEMA solution equilibrated with $0.1\,M\ Nd(NO_3)_3 + 0.1\,M\ HNO_3$, it was not possible to perform the measurements because of the formation of a precipitate during sample preparation. However, the organic phases contacted with the $1\,M\ HNO_3$ aqueous phase provided the same results for both HDHP and HDEHP. We assume this to also hold for the organic phase prepared at the lower aqueous HNO_3 concentration.

The ESI-MS results showed that the species formed in the organic phase are essentially the same for the two aqueous phases used to extract Nd^{3+}. The assignment of the species is reported in Table 3, where D stands for the malonamide and A for the anion of the organophosphoric acid, respectively. Nd-D and mixed Nd-D-HA species are observed (Fig. 7a). The main difference is the absence of nitrato-species at the lower acidity ($0.1\,M\ HNO_3$) in the aqueous phase. Since nitrato-species are formed when the metal nitrate is extracted by the malonamide (see equilibrium 2), this result suggests that the malonamide by itself does not contribute to neodymium extraction at low aqueous acidity. Indeed, under the conditions of low acidity and nitrate ion concentration, the diamide is a poor extractant of lanthanide cations. The $[D_xNd]^{3+}$ species (with $x = 3$ or 4) in the ESI-MS spectrum can arise from mixed complexes.

Table 3. m/z ratio and species assignment in the ESI-MS^+ data for the HDEHP-DMDOHEMA system after extraction of Nd^{3+} from I: $0.1\,M\ Nd(NO_3)_3 + 0.1\,M\ HNO_3$, or II: $0.1\,M\ Nd(NO_3)_3 + 1\,M\ HNO_3 + 2\,M\ NaNO_3$ (D stands for DMDOHEMA and HA for HDEHP)

Species	m/z	I	II
$[D_3Nd]^{3+}$	530.9	+	+
$[D_4Nd]^{3+}$	691.8	+	+
$[D_5Nd]^{3+}$	852.3	+	+
$[D_2Nd(NO_3)]^{2+}$	585.4	−	+
$[D_3Nd(NO_3)]^{2+}$	826.9	−	+
$[D_2Nd(NO_3)_2]^{+}$	1232.8	−	+
$[D_2NdA]^{2+}$	715.0	+	+
$[D_3NdA]^{2+}$	956.2	+	+
$[DNdA_2]^{+}$	1268.8	+	+
$[D_2NdA(NO_3)]^{+}$	1492.0	−	+
$[DNd(HA)A_2]^{+}$	1591.0	+	+
$[D_2NdA_2]^{+}$	1751.2	+	+

+: observed species; −: absent species

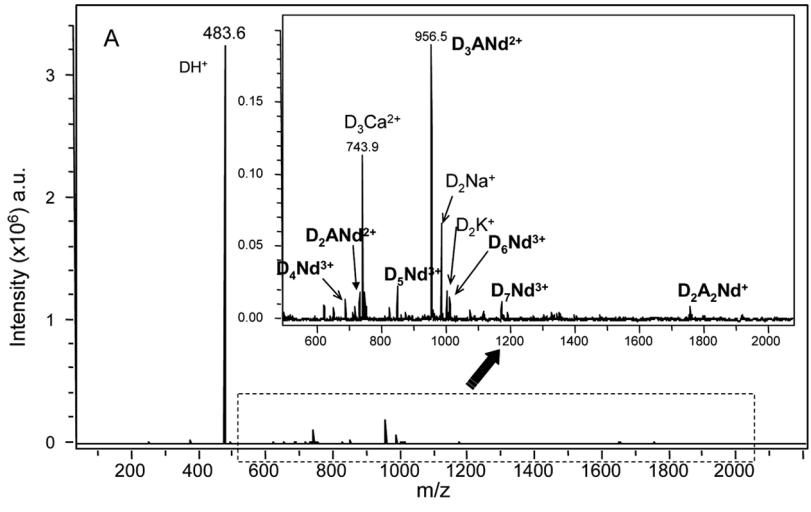

(a)

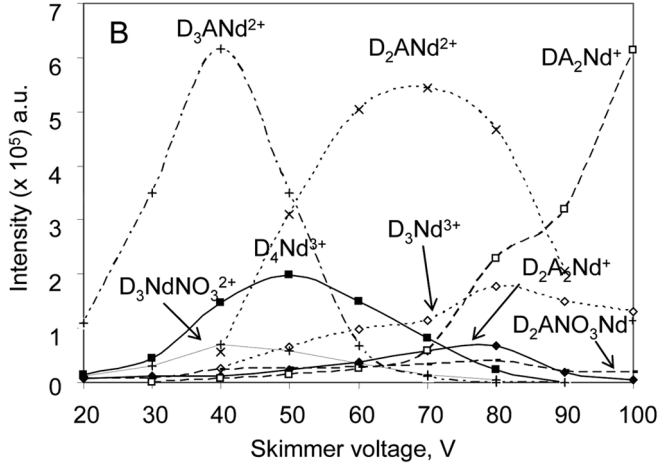

(b)

Figure 7. A. Positive ESI mass spectrum for 0.65 M DMDOHEMA + 0.3 M HDEHP in *n*-dodecane after equilibration with 0.1 M $Nd(NO_3)_3$ in 0.1 M HNO_3. D and A represent DMDOHEMA and $DEHP^-$, respectively. B. Intensity of neodymium-species as a function of cone voltage for 0.65 M DMDOHEMA + 0.3 M HDEHP in *n*-dodecane after equilibration with 0.1 M $Nd(NO_3)_3$ in 1 M HNO_3 + 2 M $LiNO_3$. D and A represent DMDOHEMA and $DEHP^-$, respectively. To simplify the plot, the species $[D_5Nd]^{3+}$, $[D_2Nd(NO_3)]^{2+}$, and $[DNd(HA)A_2]^+$ are not shown.

At higher aqueous acidity and NO_3^- concentrations, the complexes formed in the organic phase can be written as $D_xNd(NO_3)_3$ for Nd extraction by the malonamide alone, and as $D_yNdA_2(NO_3)$ or D_yNdA_3 (with $y \leq 5$) for the mixed complexes. During the ionization process and the transfer into the gas phase, the last two complexes are transformed into $[D_yNd]^{3+}$ (with $y \leq 5$), $[D_3NdA]^{2+}$, $[D_2NdA(NO_3)]^+$, $[D_2NdA_2]^+$ and $[DNd(HA)A_2]^+$.

An energy resolved mass spectrometry experiment with cone voltage variation showed that the Nd-D-HA mixed complexes predominate over the metal complexes containing only the diamide for both aqueous phase conditions. Fig. 7b presents the results obtained with the 0.1 M $Nd(NO_3)_3 + 1$ M $HNO_3 + 2$ M $NaNO_3$ aqueous phase. Increasing the cone voltage induces fragmentation of $[D_3NdA]^{2+}$ leading to $[D_2NdA]^{2+}$ by the loss of one malonamide. This fragmentation has been confirmed by MS^2 experiments. In the same way, the $[DNdA_2]^+$ species, only observed at high cone voltage, is probably formed by fragmentation of other ions.

To summarize, mixed species are formed whatever the aqueous phase acidity, and Nd-DMDOHEMA complexes are also formed at higher acidity. This is consistent with the fact that, at high aqueous phase acidities, the diamide is a good extractant for Ln(III).

VPO

VPO measurements with mixtures of solutes can be used to investigate the formation of mixed species. However, caution is needed in interpreting the results, because mixed species may form without changing the total number of particles in solution. In our specific system, for example, if the HDHP · DMDOHEMA mixed species were formed at the expense of HDHP dimers, the new species would not be detected by VPO measurements.

With this caveat in mind, VPO data for *n*-pentane solutions containing increasing concentrations of HDHP (from 0.001 to 0.3 M) and constant 0.1 or 0.3 M DMDOHEMA were obtained after equilibration with water, and compared with those for the single extractants. The results showed a significant decrease of the number of particles in solution for the mixtures containing 0.3 M DMDOHEMA, indicating the formation of mixed extractant species, at least under this condition.

The results, together with those for the single extractants, are shown in Fig. 8a as number-average aggregation number, n_{av}, vs. total solute concentration. The increased slopes for the n_{av} values for the extractant mixtures indicate that the n_{av} values for the mixtures are not equal to the average of the values for the single extractants (e.g., for 0.3 M

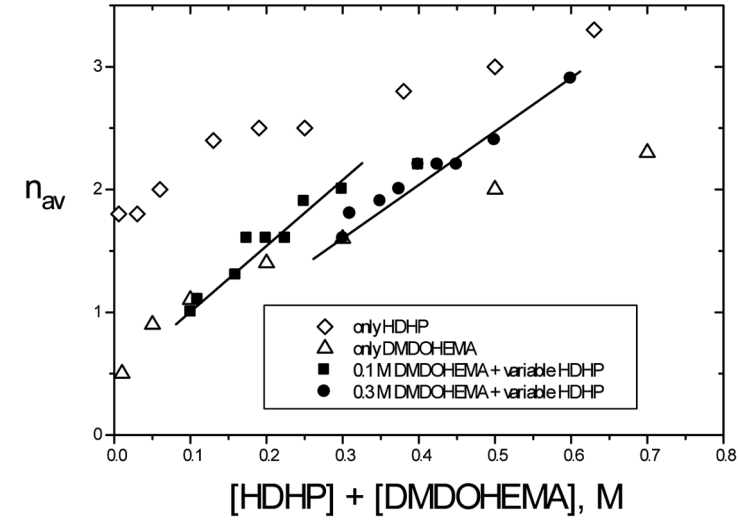

(a)

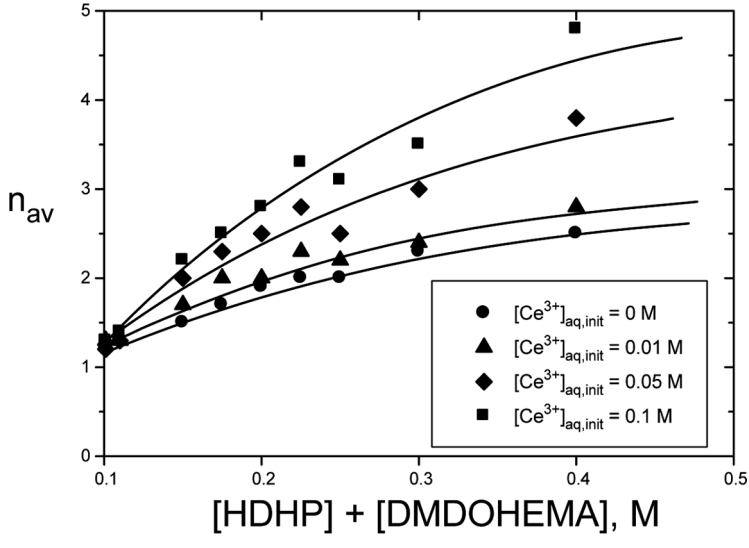

(b)

Figure 8. A. Number-average aggregation number, n_{av}, as a function of total extractant concentration for only HDHP, only DMDOHEMA, and 0.1 M or 0.3 M DMDOHEMA in *n*-pentane in the presence of increasing concentrations of HDHP after equilibration with water at 24°C. B. n_{av} for 0.1 M DMDOHEMA in *n*-pentane in the presence of increasing concentrations of HDHP after equilibration with 0.1 M HNO_3 + 2.9 M $NaNO_3$ + 0.01, 0.05 or 0.1 M $Ce(NO_3)_3$ at 24°C.

HDHP + 0.3 M DMDOHEMA, $n_{av} = 3$, whereas for 0.6 M DMDOHEMA, $n_{av} = 2.1$, and for 0.6 HDHP M, $n_{av} = 3.1$). This result suggests the presence in solution of mixed HDHP-DMDOHEMA aggregates.

Figure 8b shows VPO data obtained for 0.1 M DMDOHEMA in the presence of increasing concentrations of HDHP in *n*-pentane after extraction of Ce^{3+} from aqueous solutions under conditions favorable for metal extraction by both extractants (2) (low acidity, i.e., pH = 1, for HDHP, and high nitrate ion concentration, i.e., 3 M, for DMDOHEMA). The results demonstrate that macroconcentrations of Ln(III)'s in the organic phase strongly promote aggregation. Water analyses in the organic phases of Fig. 8b indicated that the extraction of water by the extractant mixtures is inversely proportional to that of the metal ion, and that the sum of the metal and water concentrations in the organic phase is practically constant. This suggests that each cation transferred into the organic phase replaces a water molecule in the extractant aggregate.

SAXS

Various HDHP-DMDOHEMA mixtures in *n*-dodecane were used to determine the effect of a number of parameters, i.e., the acidity of the aqueous phase (with or without Ln(III) or Am(III) cations), the extractant concentrations, the nature and concentration of the cation, on the size of the polar core of the organic phase micelles.

Samples 11 through 13 in Table 1 indicate that an increase of the HNO_3 and water concentrations in the organic phase brings about an increase of the size of the polar core of the aggregates. The SAXS data for samples 11, 12, and 13 are shown in Fig. 9a. The diameter of the polar core, d_p, increases from 11 to 14 Å as the organic phase HNO_3 concentration increases from 0 to 0.20 to 0.47 M (corresponding to 0.1, 1, and 3 M HNO_3 in the aqueous phase, respectively).

The presence of Nd(III) or Am(III) in the organic phase (samples 16 through 22 in Table 1) does not modify the tendency of the polar core size to increase with the extracted amounts of acid and water. The results obtained for the Am(III) containing samples 20, 21, and 22 exhibit the same behavior as the samples without metal, with d_p increasing from 10 to 14 Å. The SAXS data for the Am(III) samples are shown in Fig. 9b and illustrate the increase of the scattering intensity upon metal extraction from 0.1, 1, and 3 M aqueous HNO_3. The Nd(III) case (samples 16 and 19) is similar: d_p increases from 10.6 to 14.1 Å when the organic HNO_3 concentration increases from zero to 0.60 M (0.1 and 3 M aqueous HNO_3, respectively). Similar results were obtained after

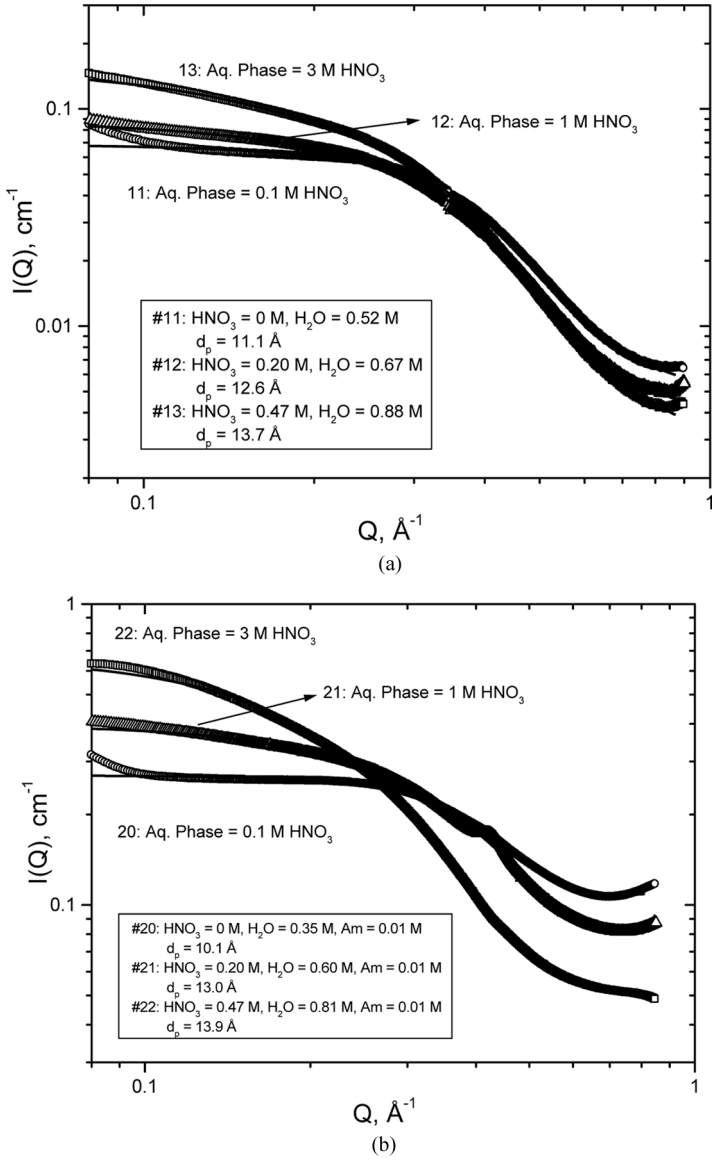

Figure 9. A. SAXS data and interacting spheres fit for 0.3 M HDHP + 0.7 M DMDOHEMA in *n*-dodecane after equilibration with 0.1 M, 1 M and 3 M HNO_3 (samples 11, 12 and 13 in Table 1). B. SAXS data and interacting spheres fit for 0.3 M HDHP + 0.7 M DMDOHEMA in *n*-dodecane after equilibration with 0.1 M, 1 M and 3 M HNO_3 containing 0.01 M $Am(NO_3)_3$ (samples 20, 21 and 22 in Table 1).

extraction of Ce(III) and Eu(III) (samples 23 and 24 in Table 1), indicating that the nature of the extracted metal species has no effect on the organic phase aggregation of the extractants.

A comparison of the scattering in Fig. 9a and b shows that the intensities are higher for the Am(III) containing samples, in spite of the very similar values of the polar core sizes obtained for metal free samples under the same extraction conditions. This is probably due to the increased contrast created by the much higher electron density in the Am-containing polar cores of the reverse micelles than in metal-free particles.

SANS

Preliminary experiments provided an important clue about the formation of HDHP-DMDOHEMA mixed reverse micelles in the organic phase. The amount of water extracted by 0.3 M HDHP + 0.7 M DMDOHEMA in *n*-dodecane under the same aqueous phase conditions (i.e., 0.1 M HNO_3, no metal ions) is much higher than the sum of the amounts of water extracted by the single components of the mixture (0.52 M, vs. 0.05 M for HDHP and 0.3 M for DMDOHEMA). This synergistic water extraction strongly suggests the formation of reverse micelles capable of increased water solubilization in their polar core.

To investigate the size and the average composition of the mixed reverse micelles, SANS data were collected for a series of samples containing both extractants after extraction of $Nd(NO_3)_3$ under a variety of conditions, including changes in the aqueous phase acidity, metal concentration, and extractant concentrations. In one case $Nd(NO_3)_3$ was replaced with $Ce(NO_3)_3$. The composition of the SANS samples and the major results from the Baxter model fit are collected in Table 2, samples 5 through 16. The weight-average aggregation numbers for HDHP and DMDOHEMA in the micelle, $n_{w,av,HDHP}$ and $n_{w,av.DMDOHEMA}$, were calculated assuming that the volume of the hydrophobic shell of the micelle is occupied by the nonpolar parts of HDHP and DMDOHEMA in proportion to the analytical concentration of the two extractants in the organic phase.

The effect of the aqueous acidity on the extractants organization in a 0.3 M HDHP + 0.7 M DMDOHEMA organic phase upon $Nd(NO_3)_3$ extraction from 0.1 and 1 M HNO_3 can be seen by comparing samples 5 and 6 in Table 2 and in Fig. 10a. The increased HNO_3 concentration in the organic phase is accompanied by swelling of the micellar polar core (from 12 to 15 Å diameter), in agreement with the results from the SAXS data, and of the whole micelle (from 21 to 24 Å diameter). The $n_{w,av}$

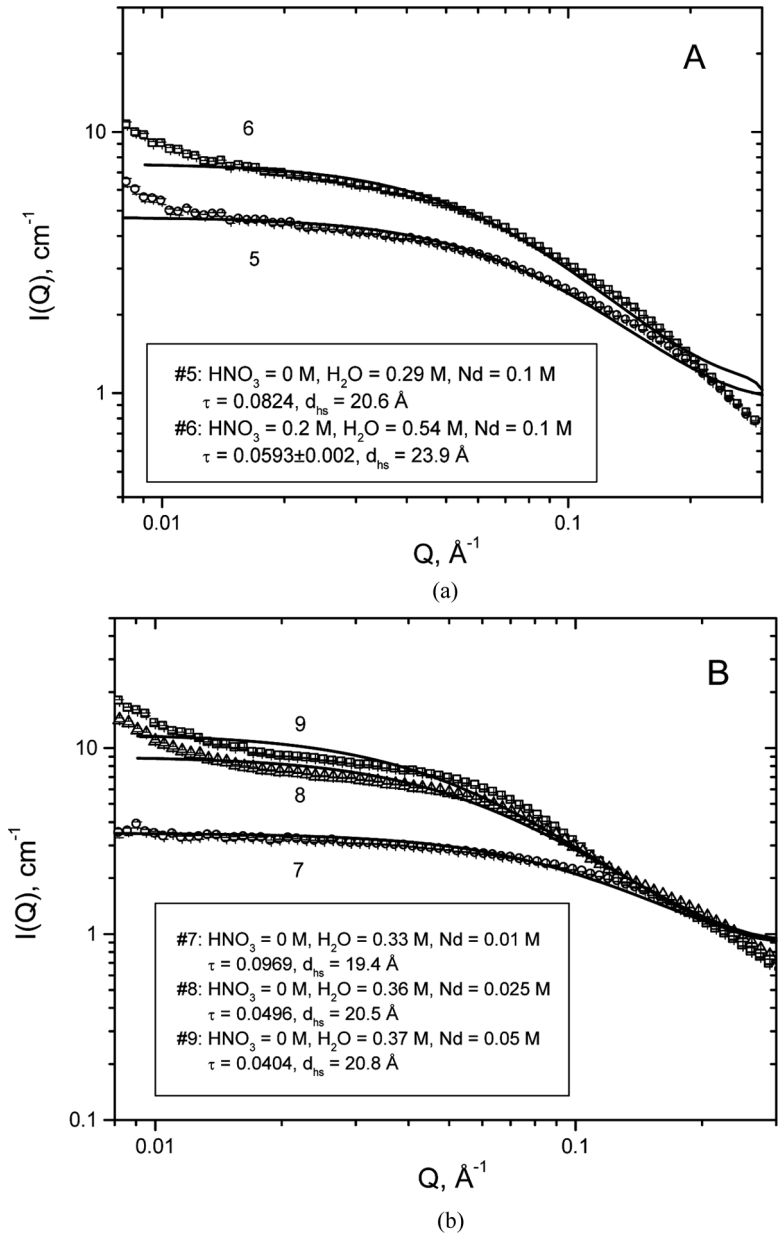

Figure 10. A. SANS data and Baxter model fit for 0.3 M HDHP + 0.7 M DMDOHEMA in deuterated *n*-dodecane after extraction of $Nd(NO_3)_3$ from 0.1 and 1 M HNO_3 (samples 5 and 6 in Table 2). B. SANS data and Baxter model fit for 0.3 M HDHP + 0.7 M DMDOHEMA in deuterated *n*-dodecane after extraction of increasing amounts of $Nd(NO_3)_3$ from 0.1 M HNO_3 (samples 7, 8, and 9 in Table 2).

values are ~ 2 for HDHP and ~ 5 for DMDOHEMA. This result is in good agreement with our previous conclusion that mixed species containing two HDHP and five DMDOHEMA molecules were needed to explain metal distribution data (2).

The effect of increasing metal concentration in the 0.3 M HDHP + 0.7 M DMDOHEMA solution is illustrated by samples 7, 8, and 9 in Table 2 and Fig. 10b. $Nd(NO_3)_3$ was extracted from 0.1 M HNO_3 (no co-extraction of HNO_3). A fivefold increase of the metal concentration in the organic phase is accompanied by only a minor increase of the size of the micelles and their polar core. Similar results were provided by the SAXS data. The mixed extractant aggregates contain 2 and 4 molecules of HDHP and DMDOHEMA, respectively. It is interesting to note that although the size of the micellar polar core for the samples in question does not change much, the energy of intermicellar attraction increases significantly, as it should be expected based on the higher concentrations of trivalent cations in the micellar core. Accordingly, the steep increase of the scattering intensity at very low Q values for samples 8 and 9 in Fig. 10b indicates that the extraction systems are close to the critical point of organic phase splitting.

In an attempt to discriminate between the two extractants in the mixed aggregates, some samples were prepared using deuterated HDHP (D-HDHP). In mixed aggregates containing DMDOHEMA and D-HDHP dissolved in deuterated *n*-dodecane, the D-HDHP should be practically invisible, and the scattered neutrons should highlight only the micellar volume occupied by the hydrogenous DMDOHEMA. Sample 10 in Table 2 and Fig. 11a was prepared under the same conditions as for sample 5 except that D-HDHP was used for sample 10. Both the d_{hs} and d_p values are essentially the same for samples 10 and 5, indicating that under the conditions used for the two samples, the supramolecular organization of the aggregates is dominated by the bulkier and larger DMDOHEMA. In the case of sample 11, the extraction of $Nd(NO_3)_3$ was performed using the same conditions as for sample 10, with the exception that 0.1 M HNO_3 in D_2O was used as the aqueous phase. This produced lower scattering intensities as compared to sample 10 (Fig. 11a). However, by taking into account the changes in the contrast factor due to the presence of D_2O instead of H_2O in the organic phase, the results of the calculations essentially confirmed those for sample 10.

The effect of the extractant concentrations in *n*-dodecane on the organization of the mixed aggregates is shown by samples 12, 13, and 14 in Table 2. In these samples, the HDHP to DMDOHEMA concentration ratio was 6, 1, and 0.14, respectively. The extraction of 0.05 M $Nd(NO_3)_3$ was effected under the same aqueous phase conditions (0.1 M HNO_3). Although the samples are not strictly comparable because

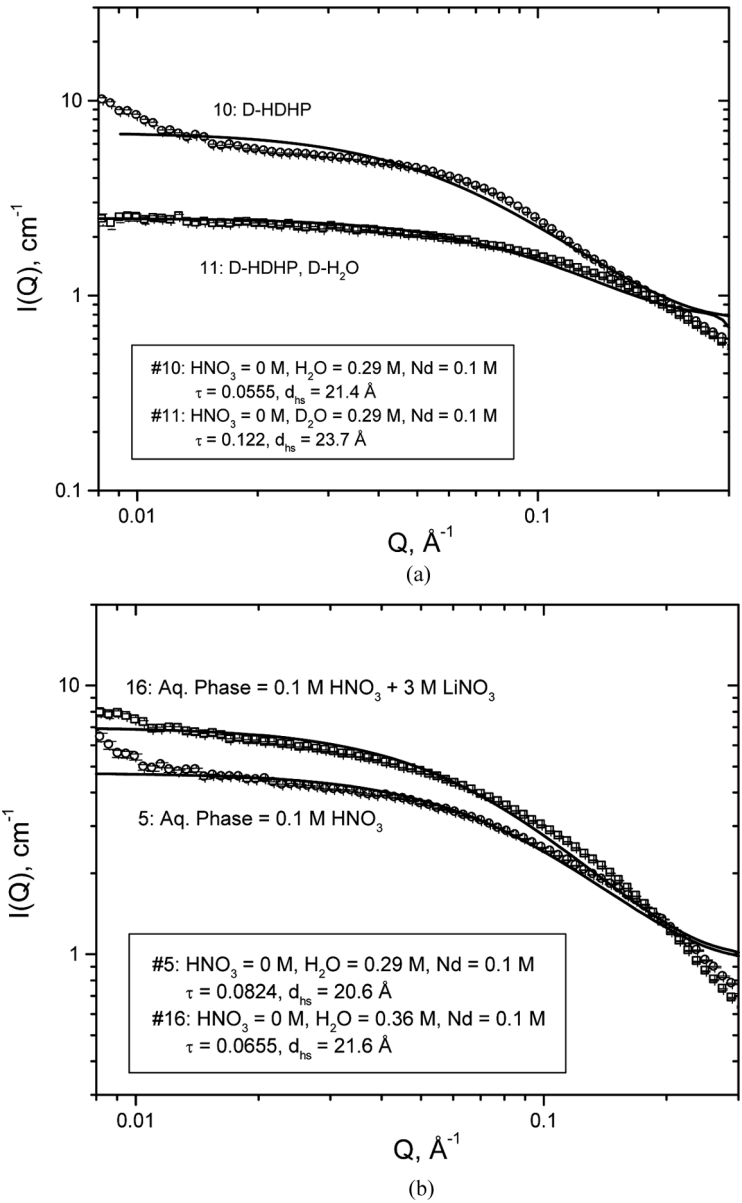

Figure 11. A. SANS data and Baxter model fit for 0.3 M deuterated HDHP + 0.7 M DMDOHEMA in deuterated *n*-dodecane after extraction of $Nd(NO_3)_3$ from 0.1 HNO_3 in H_2O (sample 10) or D_2O (sample 11 in Table 2). B. SANS data and Baxter model fit for 0.3 M HDHP + 0.7 M DMDOHEMA mixtures in deuterated *n*-dodecane after extraction of $Nd(NO_3)_3$ from 0.1 M HNO_3 (samples 5) or 0.1 M HNO_3 + 3 M $LiNO_3$ (sample 16 in Table 2).

the amount of extracted water increases with the DMDOHEMA concentration, the particle sizes and aggregation numbers in Table 2 indicate that the extractant in excess dominates the aggregation.

Sample 15 in Table 2 was prepared by extracting $Ce(NO_3)_3$ under the same conditions used for the extraction of $Nd(NO_3)_3$ in sample 7. The close similarity of results obtained for samples 15 and 7 provides evidence that the nature of the extracted cation does not play a major role in determining the aggregation of the HDHP-DMDOHEMA extractant mixtures.

Finally, Fig. 11b compares the results for sample 5 with those obtained for sample 16 in Table 2. The two samples differ in the type of aqueous phase used for the extraction of $Nd(NO_3)_3$, i.e., 0.1 M HNO_3 vs. 0.1 M $HNO_3 + 3$ M $LiNO_3$. Contrary to HNO_3, $LiNO_3$ is not extracted by the 0.3 HDHP + 0.7 M DMDOHEMA mixture. In spite of a somewhat higher scattering intensity for sample 16, the results for the two samples in Table 2 are very similar. It is, however, remarkable that the $n_{w,av,HDHP}$ and $n_{w,av.DMDOHEMA}$ values for sample 16 (~ 2 and ~ 5, respectively) closely match the results of our previous solvent extraction study under the same aqueous phase conditions (2).

CONCLUSIONS

Di-*n*-hexylphosphoric acid (HDHP) in *n*-alkane diluents forms primarily dimeric aggregates in analogy with the general behavior of dialkylphosphoric acids. Upon extraction of macroconcentrations of Ln(III) cations from nitric acid solutions, various metal-containing species, including dinuclear ones, are formed, the most important of which has the composition $M(DHP)_3(HDHP)_3(H_2O)$, where M stands for a generic Ln(III) or An(III) cation. These species exist as spherical aggregates of the reverse micelle type with a polar core diameter of ~ 7 Å and a total diameter of ~ 11 to ~ 15 Å, depending on metal loading.

The aggregation of *N,N′*-dimethyl-*N,N′*-dioctylhexylethoxymalonamide (DMDOHEMA) in *n*-alkane diluents is a progressive phenomenon, with an average aggregation number of ~ 2 in the 0.2 to 0.6 M range and aggregates with an average aggregation number, n_{av}, of ~ 4, forming at higher concentrations. Water extraction by DMDOHEMA increases sharply after the onset of aggregation, which can be taken as an indicator of extractant micellization. An increase of the DMDOHEMA n_{av} (up to ~ 6) is brought about by extraction of either HNO_3 or lanthanide nitrates. SAXS and SANS measurements showed that the metal loaded DMDOHEMA aggregates can be considered as interacting spheres with a polar core diameter between ~ 11 and ~ 16 Å, depending on sample

composition, a total diameter of up to $\sim$25 Å, and a weight-average aggregation number, $n_{w,av}$, of $\sim$9.

The results of the measurements performed in this work provided strong evidence for the formation of mixed aggregates when mixtures of HDHP and DMDOHEMA are used for the extraction of trivalent Ln and An cations. For example, VPO data showed that the number of particles in a mixture of the two extractants in contact with water is significantly lower than that expected from the contribution of the two single extractants. Also, synergistic water extraction was observed by comparing water extraction for a mixture of extractants with that for the single components. The formation of mixed aggregates upon metal extraction was further confirmed by ESI-MS measurements which identified, among others, species containing 2 organophosphorus acid and several diamide molecules (up to 5) per metal center.

SAXS and SANS measurements for mixtures of HDHP and DMDOHEMA in *n*-dodecane under a variety of conditions, i.e., by varying extractant concentrations, aqueous phase acidity and ionic strength, type of cation extracted, and the level of loading of the organic phase, concurred in providing information on the size and composition of the mixed aggregates. Within the limits and approximations of the models used for the interpretation of the data, the results consistently indicated that the mixed reverse micelles have a diameter between 19 and 24 Å with a polar core diameter of 10 to 14 Å, the upper values being obtained for micelles swollen by the extraction of HNO_3 and water. The nature of the metal cation and its concentration in the organic phase have little effect on the micelle morphology.

The composition of the mixed micelles was estimated from the SANS data. For 0.3 M HDHP + 0.7 M DMDOHEMA in *n*-dodecane, a condition of particular interest for process application, the most recurrent micellar composition is 2 HDHP and 4 or 5 DMDOHEMA molecules. This composition corresponds to that arrived at in our previous work based solely on metal and extractant distribution data. The results from our distribution and supramolecular chemistry investigations, thus, support each other and confirm the formation of mixed reverse micelles in HDHP–DMDOHEMA extractant mixtures.

ACKNOWLEDGMENTS

We thank the staff of the Chemistry Division of ANL for assistance in obtaining the first-of-kind SAXS data of Am samples; Dr. M. P. Jensen (ANL, CHM) for providing a purified stock solution of ^{243}Am; Dr. S. Seifert (ANL, APS) for generous support at the Sector 12 beam lines;

and Denis Wozniak (ANL, IPNS) for help provided during the SANS measurements. This work was supported by the U. S. Department of Energy, Office of Basic Energy Science, Division of Chemical Sciences, Biosciences and Geosciences, under contract No DE-AC02–06CH11357 (for the part performed at Argonne National Laboratory); and by the CEA, DRCP/SCPS, for the part performed at Marcoule. This collaboration was realized in the framework of the CEA-DOE agreement (C5096).

REFERENCES

1. Baron, P.; Hérès, X.; Lecomte, M.; Masson, M. (2001) Separation of minor actinides: the DIAMEX-SANEX concept. *Conference on Future Nuclear Systems, Global'2001*, Paris, France, Sept. 9–13.
2. Gannaz, B.; Chiarizia, R.; Antonio, M.R.; Hill, C.; Cote, G. (2007) Extraction of Lanthanides(III) and Am(III) by Mixtures of Malonamide and Dialkylphosphoric Acid. *Solvent Extr. Ion Exch.*, *25*: 313–337.
3. Marcus, Y.; Kertes A.S. (1969) *Ion Exchange and Solvent Extraction of Metal Complexes*; Wiley- Interscience: New York, NY, 521–551.
4. Kolarik, Z. (1982) Critical evaluation of some equilibrium constants involving acidic organophosphorus extractants. *Pure Appl. Chem.*, *54*: 2593–2674.
5. Kolarik, Z.; Sistkova, N.A.; Hejna, J. (1969) The formation of complexes in systems involving acidic organophosphorus extractants. *In Solvent Extraction Research*, Kertes, A.S; Marcus, Y.; Eds., Wiley-Interscience: New York, NY, 59–67.
6. Ulyanov, V.S.; Sviridova, R.A. (1970) Determination of the values of the dimerization, distribution, and acid dissociation constants of dialkylphosphoric acids and the constants of association with tributyl phosphate and trioctylphosphine oxide in various diluents. *Soviet Radiochem.*, *12*: 41–53.
7. Tian, Q.; Hughes, M.A. (1994) The mechanism of extraction of HNO_3 and neodymium with diamides. *Hydrometallurgy*, *36*: 315–330.
8. Erlinger, C.; Belloni, L.; Zemb, Th.; Madic, C. (1999) Attractive interactions between reverse aggregates and phase separation in concentrated malonamide extractant solutions. *Langmuir*, *15*: 2290–2300.
9. Martinet, L. (2006) Organisation supramoléculaire des phases organiques de malonamides du procédé d'extraction DIAMEX. Report CEA-R-6105.
10. Berthon, L.; Martinet, L.; Testard, F.; Madic, C; Zemb,T. (2007) Solvent penetration and sterical stabilization of reverse aggregates based on diamex process extracting molecules: Consequences on the Third Phase Formation. *Solv. Extr. Ion Exch.*, *25*: 545–576.
11. Gannaz, B.; Antonio, M.R.; Chiarizia, R.; Hill, C.; Cote, G. (2006) Structural study of trivalent lanthanide and actinide complexes formed upon solvent extraction. *Dalton Trans.*, *38*: 4553–4562.
12. Traeger, J.C. (2000) Electrospray mass spectrometry of organometallic compounds. *Int. J. Mass Spectrom.*, *200*: 387–401.

13. Di Marco, V.B.; Bombi, G.C. (2006) Electrospray mass spectrometry (ESI-MS) in the study of metal-ligand solution equilibria. *Mass Spectrometry Reviews*, *25*: 347–379.
14. Krabbe, J.G.; de Boer, A.R.; van der Zwan, G.; Lingeman, H. (2007) Metal-complex formation in continous-flow ligand-exchange reactors studied by electrospray mass spectrometry. *J. Am. Soc. Mass Spectrom.*, *18*: 707–713.
15. Colette, S.; Amekraz, B.; Madic, C.; Berthon, L.; Cote, G.; Moulin, C. (2002) Use of electrospray mass spectrometry (ESI-MS) for the study of europium (III) complexation with bis(dialkyltriazinyl)pyridines and its implication in the design of new extracting agent. *Inorg. Chem.*, *41*: 7031–7041.
16. Colette, S.; Amekraz, B.; Madic, C.; Berthon, L.; Cote, G.; Moulin, C. (2003) Trivalent lanthanide interactions with a terdentate bis(dialkyltriazinyl)-pyrdine ligand studied by electrospray ionisation mass spectrometry. *Inorg. Chem.*, *42*: 2215–2226.
17. Crowe, M.C.; Kapoor, R.N.; Cervantes-Lee, F.; Parkanyi, L.; Schulte, L.; Pannell, K.H.; Brodbelt, J.S. (2005) Investigating bidentate and tridentate carbamoylmethylphosphine oxide ligand interactions with rare-earth elements using electrospray ionization quadrupole ion trap mass spectrometry. *Inorg. Chem.*, *44*: 6415–6424.
18. Lamouroux, C.; Moulin, C.; Tabet, J. C.; Jankowski, C. K. (2000) Characterization of zirconium complexes of interest in spent nuclear fuel reprocessing by electrospray ionization mass spectrometry. *Rapid Commun. Mass Spectrom.*, *14*: 1869–1877.
19. Lamouroux, C.; Rateau, S.; Moulin, C. (2006) Use of electrospray ionization mass spectrometry for the study of Ln(III) complexation and extraction speciation with calixarene-CMPO in the fuel partitioning concept. *Rapid Commun. Mass Spectrom.*, *20*: 2041–2052.
20. Leclerc, E.; Guillaumont, D.; Guilbaud, P.; Berthon L. Mass spectrometry and theoretical investigation of di-alkylphosphoric acid – lanthanide complexes. *Radiochimica Acta*, submitted.
21. Buch, A.; Pareau, D.; Stambouli, M.; Durand, G. (2001) Solvent extraction of nickel(II) by 2-ethylhexanal oxime from various aqueous solutions. *Solvent Extr. Ion Exch.*, *19*: 277–299.
22. Buch, A.; Stambouli, M.; Pareau, D.; Durand, G. (2002) Solvent extraction of nickel(II) by mixture of 2-ethylhexanal oxime and bis(2-ethylhexyl) phosphoric acid. *Solvent Extr. Ion Exch.*, *20*: 49–66.
23. Beno, M.A.; Engbretson, M.; Jennings, G.; Knapp, G.S.; Linton, J.; Kurtz, C.; Rutt, U.; Montano, P.A. (2001) BESSRC-CAT bending magnet beamline at the advanced photon source. *Nucl. Instrum. Methods Phys. Res. A*, *467*: 699–702.
24. Seifert, S.; Winans, R. E.; Tiede, D. M.; Thiyagarajan, P. (2000) Design and performance of a ASAXS instrument at the advanced photon Source. *J. Appl. Crystallogr.*, *33*: 782–784.
25. Guinier, A.; Fournet, G. (1955) *Small-angle scattering of x-rays*; Wiley: New York.

26. Thiyagarajan, P. (2003) Characterization of materials of industrial importance using small-angle scattering techniques. *J. Appl. Crystallogr.*, *36*: Part 3 Sp. Iss. 1, 373–380.
27. Thiyagarajan, P.; Urban, V.; Littrell, K.C.; Ku, C.; Wozniak, D.G.; Belch, H.; Vitt, R.; Toeller, J.; Leach, D.; Haumann, J.R.; Ostrowski, G.E.; Donley, L.I.; Hammonds, J.; Carpenter, J.M.; Crawford, R.K. (1998) The performance of the small-angle diffractometer SAND at IPNS, in *ICANS XIV, The Fourteenth Meeting of the International Collaboration on Advanced Neutron Sources*, Starved Rock Lodge: Utica, IL, June 14–19, vol. 2, 864–878.
28. Thiyagarajan, P.; Epperson, J.E.; Crawford, R.K.; Carpenter, J.M.; Klippert, T.E.; Wozniak, D.G. (1997) The time-of-flight small–angle diffractometer at IPNS, Argonne National Laboratory. *J. Appl. Cryst.*, *30*: 280–293.
29. Porod, G. (1982) General Theory, Chapter 2 in *Small Angle X-ray Scattering*, Glatter, O., Kratky, O. Eds.; Academic Press: New York, NY, 17–51.
30. Baxter, R.J. (1968) Percus-yevick equation for hard spheres with surface adhesion. *J. Chem. Phys.*, *49*: 2770–2774.
31. Chiarizia, R.; Jensen, M.P.; Rickert, P.G.; Kolarik, Z.; Borkowski, M.; Thiyagarajan, P. (2004) Extraction of zirconium nitrate by TBP in *n*-octane: Influence of cation type on third phase formation according to the "sticky spheres" model. *Langmuir*, *20*: 10798–10808.
32. Jensen, M.P.; Chiarizia, R.; Urban, V.; Nash, K.L. (2001) Aggregation of the neodymium complexes of HDEHP, Cyanex 272, Cyanex 302 and Cyanex 301 in toluene. *Proceedings of the International Symposium NUCEF 2001, Scientific Bases for Criticality Safety, Separation Process and Waste Disposal,* Japan Atomic Energy Research Institute (JAERI), Tokai-mura, Ibaraki, Japan, Oct. 31–Nov. 2, JAERI-Conf, 2002–004, March 200, 281–288.
33. Nave, A.; Mandin, C.; Martinet, L.; Berthon, L.; Testard, F.; Madic, C.; Zemb, Th. (2004) Supramolecular organization of tri-*n*-butyl phosphate in organic diluent on approaching third phase transition. *Phys. Chem. Chem. Phys.*, *6*: 799–808.
34. Chiarizia, R.; Nash, K.L.; Jensen, M.P.; Thiyagarajan, P.; Littrell, K.C. (2003) Application of the baxter model for hard-spheres with surface adhesion to SANS data for the U(VI) – HNO_3, TBP – *n*-dodecane system. *Langmuir*, *19*: 9592–9599.
35. Chiarizia, R.; Jensen, M.P.; Borkowski, M.; Thiyagarajan, P.; Littrell, K.C. (2004) Interpretation of third phase formation in the Th(IV)-HNO_3, TBP-*n*-octane system with baxter's "sticky spheres" model. *Solvent Extr. Ion Exch.*, *22*: 1–27.
36. Chiarizia, R; Rickert, P.G.; Stepinski, D.; Thiyagarajan, P.; Littrell, K.C. (2006) SANS study of third phase formation in the HCl-TBP-*n*-octane system. *Solvent Extr. Ion Exch.*, *24*: 125–148.
37. Pedersen, J.S. (1997) Analysis of small-angle scattering data from colloids and polymer solutions: Modeling and least-squares fitting. *Adv. Colloid Interface Sci.*, *70*: 171–210.